Delta(1232) and Nucleon Spectral Functions in Hot Hadronic Matter

H. van Hees[1] and R. Rapp[1]

[1]*Cyclotron Institute and Physics Department, Texas A&M University, College Station, Texas 77843-3366*
(Dated: October 25, 2004)

Modifications of $\Delta(1232)$ and nucleon spectral functions at finite temperature and baryon density are evaluated in terms of resonant scattering off thermal pions, as well as a renormalization of the vacuum Δ-width including vertex corrections. The interactions are based on effective Lagrangians of pions and baryon resonances, with underlying parameters (coupling constants and form factors) determined by the elastic πN scattering phase shift in the isobar channel, and by empirical decay branchings of excited resonances. Pion modifications are included via interactions in a pion gas, as well as standard Δ- and nucleon-hole excitations in nuclear matter. In hot hadronic matter, under conditions resembling thermal freezeout at the Relativistic Heavy-Ion Collider (RHIC), the Δ exhibits a significant broadening of $\sim$65 MeV together with a slight upward peak shift of 5-10 MeV, in qualitative agreement with preliminary data from the STAR collaboration.

PACS numbers: 25.75.-q,21.65.+f,12.40.-y

I. INTRODUCTION

In strong interactions at low and intermediate momentum transfer the relevant degrees of freedom are associated with colorless hadrons. Whereas their interactions are constrained by the approximate chiral symmetry (CS) in the two-flavor sector of Quantum Chromodynamics (QCD), their mass spectrum is largely governed by the spontaneous breaking of CS (SBCS) in the QCD vacuum. At temperatures $T \simeq$ 150-200 MeV, CS is expected to be restored [1], implying substantial modifications of the hadronic spectrum close to the critical temperature. Pertinent medium modifications of hadrons are hoped to be identified by creating hot and dense nuclear matter in high-energetic collisions of heavy nuclei.

In recent years, intense theoretical efforts have been devoted to understand in-medium properties of especially vector mesons, which are rather directly accessible in heavy-ion experiments through decays into dileptons, emitted throughout the hot and dense phases of the collision with negligible final-state interactions (for a review, see, e.g., Ref. [2]). Baryonic effects have been found to be of particular importance in accounting for the large excess production of lepton pairs, observed in Pb-Au collisions [3, 4], at invariant masses below the vacuum ρ-mass. Consequently, towards a more complete picture, in-medium effects of the baryon spectrum itself deserve further investigation.

In the present article we calculate modifications of the nucleon (N) and $\Delta(1232)$ particles in a hot and dense medium within an effective quantum-field theoretical hadronic model coupled with standard many-body techniques. Besides their (indirect) role in dilepton production, Δ properties in heavy-ion collisions are accessible via resonance spectroscopy, i.e., mass and width changes in the line shapes of πN invariant-mass spectra [5, 6, 7, 8]. In-medium Δ spectral function to date were mostly evaluated for cold nuclear matter [9, 10, 11, 12, 13, 14], with few exceptions [15, 16]. Here we go beyond the latter works by performing a more detailed treatment of its pion-nucleon cloud at finite temperature including vertex corrections, as well as resonance excitations induced by thermal pions. Also, thermal self-energies of the nucleon beyond the Δ contribution are, to our knowledge, assessed for the first time [17, 18, 19, 20]. In a more general context, the change of the baryon spectrum towards chiral restoration is an important component in the understanding of QCD phase transitions in the μ_B-T plane (μ_B: baryon chemical potential).

Our article is organized as follows: In Sec. II we introduce the hadronic interaction Lagrangians that are subsequently employed and discuss the determination of the free parameters, using vacuum scattering and decay data. In Sec. III we compute in-medium self-energies of nucleon and Δ. The latter are used in Sec. IV to evaluate N and Δ spectral properties in matter. For the Δ, we first qualitatively confront the effects of cold nuclear matter with information from nuclear photoabsorption, and then discuss both N and Δ spectral functions in hot and dense matter under conditions expected for heavy-ion experiments at various collision energies. In Sec. V we summarize and give an outlook.

II. HADRONIC INTERACTION LAGRANGIANS IN VACUUM

The central quantities of interest in our present analysis are the in-medium propagators of the two lowest-lying non-strange baryon states, nucleon and Δ. Throughout this article we employ a quasi-relativistic description of the baryon fields, i.e., use relativistic dispersion relations, $E_B^2(\vec{p}) = m_B^2 + \vec{p}^2$ (B=N, Δ, N^*, Δ^*), but neglect anti-particle contributions and additionally restrict Rarita-Schwinger spinors to their non-relativistic spin-3/2 components. Pions

are treated fully relativistic, with $\omega_\pi^2(\vec{k}) = m_\pi^2 + \vec{k}^2$. Within this approximation, the free retarded propagators for baryons and pions read

$$G_B^{(0)}(p) = \frac{1}{p_0 - E_B(\vec{p}) - \Sigma_B^{(0)}(p)} \ , \qquad G_\pi^{(0)}(k) = \frac{1}{k_0^2 - \omega_\pi^2(\vec{k}) + \mathrm{i}\eta \, \mathrm{sign}(k_0)}, \tag{1}$$

where $\Sigma_B^{(0)}(p)$ denotes the vacuum self-energy encoding the partial decay branchings of each resonance. Except for the Δ (for which a renormalization of its bare mass is accounted for via the πN loop), we use constant physical pole masses implying that only the imaginary part of $\Sigma_B^{(0)}$ is nonzero (for the nucleon, $\Sigma_B^{(0)}=0$).

A key ingredient in our description are the interaction vertices involving a pion and two baryons. The following notation is adopted below: two-component spin-1/2 fields are denoted by ψ and four-component spin-3/2 fields by Ψ; the isospin of a resonance is indicated by an appropriate subscript ("1" and "3" for $I = 1/2$ and $3/2$, respectively). The dominant coupling type is usually given by the lowest angular momentum in the pion decay (except for πNN, where s-wave interactions are neglected), but higher waves are included whenever empirically significant. Pions are represented by a real isospin triplet $\vec{\phi}$ transforming according to the fundamental SO(3) representation of the isospin group. This leads us to the following interactions [10, 21, 22, 23, 24] involving nucleons,

$$\mathscr{L}_{s,N}^{(11)} = -f\psi_1^\dagger \vec{\tau}\vec{\phi}\psi_N + \mathrm{h.c.} \tag{2}$$

$$\mathscr{L}_{p,N}^{(11)} = -\frac{f}{m_\pi}\psi_1^\dagger[(\vec{\sigma}\vec{\nabla})(\vec{\tau}\vec{\phi})]\psi_N + \mathrm{h.c.} \tag{3}$$

$$\mathscr{L}_{s,N}^{(31)} = -f\psi_3^\dagger \vec{T}\vec{\phi}\psi_N + \mathrm{h.c.}, \tag{4}$$

and $\Delta(1232)$ resonances,

$$\mathscr{L}_{s,\Delta}^{(13)} = \mathrm{i}g\Psi_1^\dagger \vec{T}^\dagger \vec{\phi}\Psi_\Delta + \mathrm{h.c.} \tag{5}$$

$$\mathscr{L}_{s,\Delta}^{(33)} = \mathrm{i}g\Psi_3^\dagger 2\vec{\Theta}\vec{\phi}\Psi_\Delta, \tag{6}$$

$$\mathscr{L}_{p,\Delta}^{(13)} = -\frac{f}{m_\pi}\psi_1[(\vec{S}^\dagger\vec{\nabla})(\vec{T}^\dagger\vec{\phi})]\Psi_\Delta + \mathrm{h.c.} \tag{7}$$

$$\mathscr{L}_{p,\Delta}^{(33)} = -\frac{f}{m_\pi}\Psi_3[(2\vec{\Sigma}\vec{\nabla})(2\vec{\Theta}\vec{\phi})]\Psi_\Delta + \mathrm{h.c.} \tag{8}$$

$$\mathscr{L}_{d,\Delta}^{(13)} = -\mathrm{i}\frac{f}{m_\pi^2}\psi_1[(\vec{S}\vec{\nabla})(\vec{S}^\dagger\vec{\nabla})(\vec{T}^\dagger\vec{\phi})]\Psi_\Delta + \mathrm{h.c.} \tag{9}$$

$$\mathscr{L}_{d,\Delta}^{(33)} = -\mathrm{i}\frac{f}{m_\pi^2}\psi_3^\dagger[(\vec{\sigma}\vec{\nabla})(\vec{S}^\dagger\vec{\nabla})(2\vec{\Theta}\vec{\phi})]\Psi_\Delta + \mathrm{h.c.} \tag{10}$$

In the above equations, the superscripts on the left-hand-side refer to the isospin content of the two baryon fields, whereas the subscripts l, N (l, Δ) indicate the angular momentum $l=s$, p and d in the πN ($\pi\Delta$) system. Furthermore, $\vec{\sigma}$ ($\vec{\tau}$) are Pauli matrices in (iso-) spin space, and $\vec{S}$ ($\vec{T}$) the pertinent $1/2\to3/2$ transition matrices (consisting of appropriate Clebsch-Gordan coefficients which project the 1-1/2 couplings onto pure 3/2 states). Finally, $\vec{\Sigma}$ ($\vec{\Theta}$) denote the (iso-) spin-3/2 (4×4-) matrices. The finite size of the vertices is accounted for by phenomenological hadronic form factors, which are of monopole type for s- and p-wave couplings (2-8), $F_{\mathrm{mon}}(|\vec{k}|) = \Lambda^2/(\vec{k}^2 + \Lambda^2)$, and of dipole type for the d-wave couplings (9) and (10), $F_{\mathrm{dip}}(|\vec{k}|) = 4\Lambda^4/(2\Lambda^2 + \vec{k}^2)^2$.

Except for πNN and $\pi N\Delta$ vertices, all $\pi B_1 B_2$ coupling constants are adjusted to the (average) empirical values of the corresponding partial $B_2 \to B_1\pi$ decays (using pole masses and widths) according to the Particle Data Group [25], together with a uniform form-factor cutoff $\Lambda_{\pi\Delta B}=500$ MeV, cf. Tab. I. Since the main focus in the present article is on spectral properties of the Δ resonance, we calculate its vacuum self-energy including a finite real part. With the interaction vertex, Eq. (8), and using free pion and nucleon propagators, its imaginary part takes the form

$$\mathrm{Im}\,\Sigma_\Delta^{(N\pi)}(M) = -\frac{f_{\pi N\Delta}}{12m_\pi^2\pi}\frac{m_N k_{\mathrm{cm}}^3}{M}F^2(k_{\mathrm{cm}})\Theta(M - m_N - m_\pi), \quad k_{\mathrm{cm}}^2 = \frac{(M^2 - m_N^2 - m_\pi^2)^2 - 4m_N^2 m_\pi^2}{4M^2} \ . \tag{11}$$

Here, we introduced an extra factor $m_N/E_N(k_{\mathrm{cm}})$ to ensure a Lorentz-invariant decay width. The real part of the self-energy is then determined by its spectral representation. Assuming the πN interaction in the 33-channel to be dominated by the Δ resonance allows to relate the self-energy to the πN elastic scattering phase shifts via

$$\tan[\delta_{33}(M)] = \frac{\mathrm{Im}\,G_\Delta(M)}{\mathrm{Re}\,G_\Delta(M)}. \tag{12}$$

Vertex	Eq.	f (g)
πNN	(3)	1.0
$\pi N\Delta$	(7)	3.2
$\pi NN(1440)$	(3)	0.779
$\pi NN(1535)$	(2)	1.316
$\pi N\Delta(1600)$	(7)	1.170
$\pi N\Delta(1620)$	(5)	0.828
$\pi \Delta N(1440)$	(7)	2.185
$\pi \Delta\Delta(1600)$	(8)	0.211
$\pi \Delta N(1520)$	(5)	0.760
	(9)	(-1.126)
$\pi \Delta N(1700)$	(9)	0.351
$\pi \Delta\Delta(1620)$	(10)	0.111
$\pi \Delta\Delta(1700)$	(6)	0.655

TABLE I: πNB and $\pi\Delta B$ vertices and coupling constants used in the present analysis.

As is well known, within this approximation a satisfactory fit to the δ_{33} phase shift [16, 26, 27] requires a low cutoff, $\Lambda_{\pi N\Delta}$=290 MeV, together with a large coupling constant, $f_{\pi N\Delta}$=3.2, and a bare mass of $m_\Delta^{(0)}$=1302 MeV [16, 26, 27]. The same cutoff will be employed for the πNN vertex with the standard value for the coupling constant, $f_{\pi NN}$=1.

Baryon-baryon interactions via t-channel meson exchange are negelcted in the present analysis. In high-temperature matter, which is our main interest here, we expect resonant meson-baryon scattering to be more important, as it was the case for earlier calculations of the pion and ρ-meson spectral functions in hot and dense matter [2].

III. IN-MEDIUM SELF-ENERGIES

With the above interaction vertices we proceed to evaluate N and Δ self-energies in hot and dense hadronic matter.

The in-medium Δ self-energy has two components. The first, and more involved one is the πN decay extended to finite temperatures and baryon densities. We employ the imaginary-time (Matsubara) formalism to calculate the corresponding $N\pi$-loop diagram according to

$$
\begin{aligned}
\Sigma_\Delta^{(N\pi)}(p) &= -\mathrm{i}\frac{f_{\pi N\Delta}^2}{3m_\pi^2}\int \frac{d^3\vec{l}}{(2\pi)^3}\frac{m_N}{E_N(\vec{l})}T\sum_{z_\nu}F^2(|\vec{k}|)\vec{k}^2 G_\pi(\mathrm{i}\omega_\kappa - \mathrm{i}z_\nu, \vec{p}-\vec{k})G_N(\mathrm{i}z_\nu, \vec{l}) \\
&= \frac{f_{\pi N\Delta}^2}{3m_\pi^2}\int \frac{\mathrm{d}^4l}{(2\pi)^4}\frac{m_N}{E_N(\vec{l})}\vec{k}^2 F_\pi^2(\vec{k}^2)\{[\Theta(k_0)+\sigma(k_0)f^\pi(|k_0|)]A_\pi(k)G_N(l) - f^N(l_0)A_N(l)G_\pi(k)\}\,,
\end{aligned}
\tag{13}
$$

where $k = p - l$ is the pion four-momentum, and $A_N = -2\,\mathrm{Im}\,G_N$ and $A_\pi = -2\,\mathrm{Im}\,G_\pi$ denote the in-medium nucleon and pion spectral function, respectively (the extra factor $m_N/E_N(\vec{l})$ ensures consistency with Eq. (11)). The thermal distribution functions are given by $f^N(l_0) = f^{\mathrm{fermi}}(l_0 - \mu_N, T)$ and $f^\pi(|k_0|) = f^{\mathrm{bose}}(|k_0|, T)\exp(\mu_\pi/T)$, with f^{fermi} and f^{bose} being the standard Fermi and Bose functions, respectively. To avoid Bose poles in the presence of finite widths for in-medium pion spectral functions, pion-chemical potentials, μ_π>0, are treated in Boltzmann approximation.

The second equality in Eq. (13) follows by using the Lehmann representation for the propagators together with an analytical continuation in the energies. Positive energies $k_0 > 0$ then correspond to outgoing pions encoding the in-medium $\Delta \to \pi N$ decay, whereas contributions with $k_0 < 0$ correspond to scattering with pions from the heat bath. The nucleon spectral function will be discussed in more detail below. The pion spectral function is based on a pion self-energy $\Sigma_\pi(k; T, \mu_\pi, \mu_N)$ that includes contributions from both finite temperatures and baryon densities. The temperature modifications are modeled by a four-point $\pi\pi$ interaction to second order in the coupling constant, corresponding to so-called sunset diagrams [28]. The value of the coupling constant is adjusted to approximately reproduce pion gas self-energies obtained from more realistic $\pi\pi$ interactions in s-, p- and d-wave [29]. The baryonic effects are calculated in terms of standard Lindhard functions for p-wave nucleon- and Δ-hole excitations at finite temperature including short-range correlations parametrized by Migdal parameters [30] (due to the soft form factors we use rather small default values g'_{11}=0.8 and $g'_{12}=g'_{22}$=0.33 [22]). As is well-known from similar evaluations of ρ-meson self-energies [31, 32] (see also Ref. [15] for an early application for the Δ), the p-wave softening of the pion dispersion relation can induce an artificial threshold enhancement due to a near vanishing of the pion group velocity.
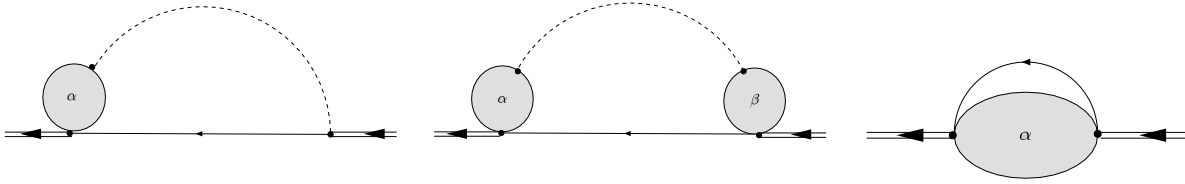
FIG. 1: Diagrammatic representation of the $\pi N \Delta$-vertex corrections (dashed lines: pion propagator, solid lines: nucleon propagator, double solid lines: $\Delta(1232)$ propagator); a blob with label α corresponds to the Lindhard function Π_α ($\alpha \in \{1, 2\}$) attached to the baryon lines with the pertinent Migdal parameters, i.e., g'_{12} for $\alpha=1$ and g'_{22} for $\alpha=2$.

This is remedied through the inclusion of vertex corrections, which, for the vector-meson case, are, in fact, required to maintain a conserved vector current. Here, we adopt a similar procedure involving four-point baryon vertices which are resummed in complete analogy to (and with the same coupling constants as) the Migdal corrections in the pion propagator. The vertex corrections amount to replacing the pion propagators in Eq. (13) by

$$\tilde{G}_\pi(k) = G_\pi(k)\{1 + g'_{12}\Pi_1(k) + g'_{22}\Pi_2 + [g'_{12}\Pi_1(k) + g'_{22}\Pi_2]^2\} + \frac{g'^2_{12}\Pi_1(k) + g'^2_{22}\Pi_2(k)}{\vec{k}^2} , \tag{14}$$

where Π_1 and Π_2 denote resummed finite-temperature Lindhard functions corresponding to Feynman diagrams with outgoing NN^{-1}-, $N\Delta^{-1}$-loops, respectively, cf. Fig.1. The vertex corrections are, in fact, closely related to the "induced interaction" as implemented in the nuclear Δ width in Ref. [10]. Here, we restrict ourselves to the longitudinal (pion-) component; the transverse part including exchange of in-medium ρ mesons will be addressed in future work.

The second component of the in-medium Δ self-energy arises from interactions with thermal pions, approximated by s-channel resonance formation. Evaluating the finite temperature part of pertinent πB loop diagrams within the Matsubara formalism leads to

$$\Sigma_\Delta^{(\pi B)}(p) = - \int\limits_{l_0 \geq p_0} \frac{\mathrm{d}^4 l}{(2\pi)^4} v_{\pi\Delta B}^2(\vec{k}) \left[f^\pi(|k_0|) A_\pi(k) G_B(l) + f^B(l_0) A_B(l) G_\pi(k) \right] . \tag{15}$$

As before, $k=p-l$ is the pion-four momentum, and $v_{\pi NB}$ are the interaction vertices (including hadronic form factors) following from the Lagrangians (5)-(10), summed (averaged) over spins and isospins of the baryon resonance B and the pion (Δ). In the baryon-resonance Green's function in-medium effects on the decay width are accounted for through thermal occupation factors, whereas modifications of the real part (due to medium effects on the various decay products), as well as possible vertex corrections, are neglected (recall that these two effects tend to compensate each other, cf. the discussion before Eq. (14) above). Also note that we suppressed the contributions of the πB loop that survive in the vacuum (technically, this is achieved by introducing the factor $\Theta(k_0)$ into the integrand). This is to ensure consistency with our fit to the free πN scattering phase shifts where such diagrams have not been included (those would not only affect the imaginary part of $\Sigma_\Delta^{(0)}$ above threshold, but also require additional mass and wave-function renormalizations through its real part).

The medium effects on the nucleon are attributed to s-channel interactions with thermal pions. Starting from the equivalent expression for the Δ, Eq.(15), we apply the same level of approximation as for the pions (encoded in the Lindhard functions), i.e., neglecting off-shell energy-dependencies in the thermal distribution functions and resonance widths. For the p-wave scattering $\pi N \to N$ and $\pi N \to \Delta$, e.g., this leads to

$$\Sigma_N^{(T)}(p) = - \int \mathrm{d}^3 \vec{l} \, \frac{\vec{k}^2 F_\pi^2}{\omega_\pi(\vec{k})} \left\{ \frac{3 f_{\pi NN}^2}{16\pi^3 m_\pi^2} \frac{f^\pi[\omega_\pi(\vec{k})] + f^N[E_N(\vec{l})]}{E_N(\vec{l}) - \omega_\pi(\vec{k}) - p_0 - \mathrm{i}\epsilon} + \frac{f_{\pi N\Delta}^2}{12\pi^3 m_\pi^2} \frac{f^\pi[\omega_\pi(\vec{k})] + f^\Delta[E_\Delta(\vec{l})]}{E_\Delta(\vec{l}) - \omega_\pi(\vec{k}) - p_0 - \mathrm{i}\Gamma_\Delta/2} \right\} . \tag{16}$$

and likewise for the other resonances listed in Table I.

Let us finally comment on the chemical potentials entering the thermal distribution functions. In high-energy heavy-ion collisions, hadron yields can be rather accurately described by a "chemical freezeout" [33], characterized by a common temperature and baryon chemical potential (depending on collision energy), with meson-chemical potentials equal to zero. In subsequent hadronic cooling, finite chemical potentials for stable mesons are required to maintain the observed hadron ratios [34]. Relative equilibrium for strong processes, e.g., $\pi\pi \leftrightarrow \rho$ or $\pi N \leftrightarrow \Delta$, then implies relations of the type $2\mu_\pi = \mu_\rho$, $\mu_N + \mu_\pi = \mu_\Delta$, which will be incorporated below.
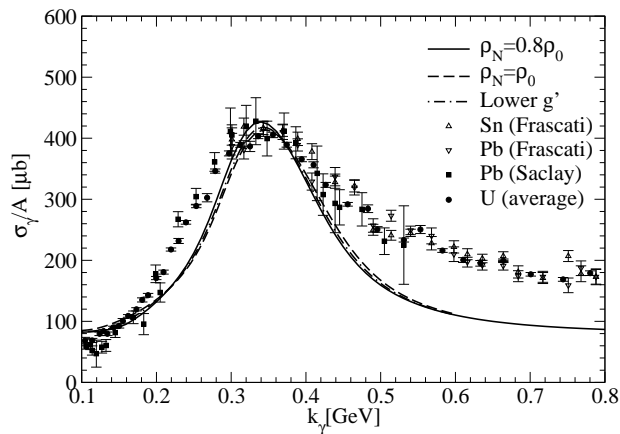
FIG. 2: Photoabsorption cross sections on nuclei [36, 37, 38, 39, 40, 41] compared to calculations employing our Δ-spectral function at finite density. Solid line: $\varrho_N=0.8\varrho_0$, $g'_{11}=0.8$, $g'_{12}=g'_{22}=0.33$, dashed line: $\varrho_N=\varrho_0$, $g'_{11}=0.8$, $g'_{12}=g'_{22}=0.33$, dash-dotted line: $\varrho_N=0.8\varrho_0$, $g'_{11}=0.6$, $g'_{12}=g'_{22}=0.2$.
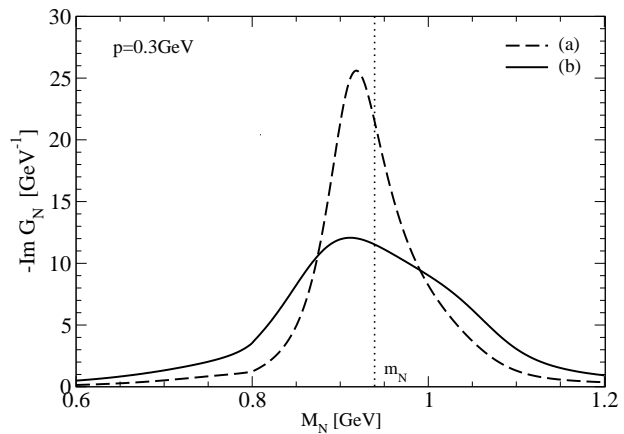
FIG. 3: Nucleon spectral function in hot hadronic matter under RHIC conditions; solid line: "chemical freezeout" with $T=180$MeV, $\varrho_N=0.68\varrho_0$ ($\mu_N=333$MeV), $\mu_\pi=0$; dashed line: "thermal freezeout" with $T=100$MeV, $\varrho_N=0.12\varrho_0$ ($\mu_N=531$MeV) and $\mu_\pi=96$MeV; the dotted line indicates the location of the free nucleon mass.

IV. NUCLEON AND Δ SPECTRAL FUNCTIONS IN MEDIUM

A. Cold Nuclear Matter

A valuable model test of the nuclear medium effects on the Δ can be performed by comparing its spectral properties to photoabsorption data on nuclei (see, e.g., Ref. [35] for a recent example). This, in particular, allows to better constrain the in-medium modifications of the pion (depending on the πNN form factor and Migdal parameters) and the impact of the $\pi N\Delta$ vertex corrections. The photoabsorption cross section can be written in terms of the photon-polarization tensor, Π_γ, as

$$\frac{\sigma^{\rm abs}_{\gamma A}}{A} = \frac{4\pi\alpha}{k}\frac{1}{\varrho_N}\frac{1}{2}\,{\rm Im}\,\Pi_\gamma(k_0=k)\ , \qquad \Pi_\gamma = \frac{1}{2}g_{\mu\nu}\Pi^{\mu\nu}\ , \tag{17}$$

where $k_0=k$ denotes the photon energy (momentum). Π_γ is evaluated via the γ-induced Δ-hole excitation which we obtain from the standard magnetic coupling [11]

$$\mathcal{L}_{\gamma N\Delta} = -\frac{f_{\gamma N\Delta}}{4\pi m_\pi}\psi^\dagger_N(\vec{S}^\dagger\times\nabla)\vec{A}T^\dagger_3\Psi_\Delta + {\rm h.c.} \tag{18}$$

The cross section on the nucleon follows from the low-density limit of Eq. (17) using the vacuum Δ propagator (we also supplemented a non-resonant constant "background" of 80 μb [22]); with a coupling constant $f_{\gamma N\Delta}=0.653$ and a (monopole-) form factor cutoff, $\Lambda_{\gamma N\Delta}=400$ MeV, the nucleon data in the Δ-resonance region are resonably well reproduced [42]. The cross section on nuclei follows with no further adjustments by using the in-medium Δ propagator, assuming an average density of $\rho_N=0.8\rho_0$ (the results are almost identical for $\rho_N=\rho_0$). Given our rather simple treatment, the agreement with the nuclear data is fair, cf. left panel of Fig. 2. The sensitivity to changes in the Migdal parameters is very moderate. The discrepancies at low energies may be due to neglecting (i) interference between resonant and non-resonant terms, (ii) direct nucleon-hole excitations, or (iii) transverse contributions in the vertex corrections of the Δ decay with medium-modified ρ mesons. Obviously, at higher energies, additional resonances need to be included.

B. Hot Hadronic Matter

We now turn to our main results, applying the model to hot and dense hadronic matter expected to be formed in heavy-ion collisions at RHIC (meson-dominated matter) and the future GSI facility (baryon-dominated matter).
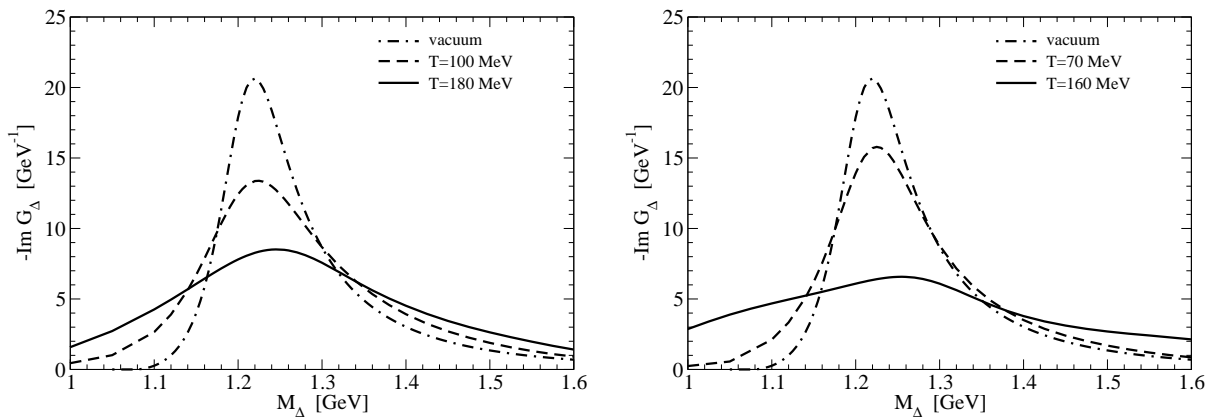
FIG. 4: Left: The in-medium spectral function of the $\Delta(1232)$ for typical conditions at RHIC, compared to the vacuum (dash-dotted line). Dashed line: T=100 MeV, ϱ_N=0.12ϱ_0 (μ_N=531 MeV), μ_π=96 MeV; solid line: T=180 MeV, ϱ_N=0.68ϱ_0 (μ_N = 333 MeV), μ_π=0. Right: The same for typical conditions, expected at the future GSI facility. Dashed line: T=70 MeV, ϱ_N=0.19ϱ_0 (μ_N=727 MeV), μ_π=105 MeV; solid line: T=160 MeV, ϱ_N=1.80ϱ_0 (μ_N=593 MeV), μ_π=0.

The nucleon-spectral function is displayed in Fig. 3 for RHIC conditions. Resonant $\pi N \rightarrow B$ scattering is found to induce an appreciable broadening (exceeding 200 MeV at the expected chemical freezeout), which, around the free nucleon mass, is to $\sim$80% due to the Δ excitation (at T=180 MeV, the shoulder at somewhat higher nucleon energies is mainly caused by the $N(1520)$ and $\Delta(1600)$ resonances). One also observes a slight attractive mass shift, induced by the higher resonance states which are located (well) above typical $N\pi$ energies.

For the $\Delta(1232)$ spectral function at RHIC (left panel in Fig. 4), about half of its width is due to baryon resonance excitations (which are additionally enhanced somewhat due to the inclusion of the in-medium pion propagator in the loop diagram). The other half of the in-medium broadening is mostly generated by the Bose enhancement factor on the pion in the πN decay. In the real part of the Δ self-energy, there is a large cancellation between the attraction generated by the baryon resonances and the repulsion induced by the medium effects on the πN loop, mostly driven by finite baryon densities (with significant contributions from the vertex corrections).

For conditions resembling thermal freezeout (dashed line in the left panel of Fig. 4), the peak position is located at about $M\simeq1.226$ GeV, and the line width has increased to $\Gamma\simeq177$ MeV, to be compared to the vacuum values of $M\simeq1.219$ GeV and $\Gamma\simeq110$ MeV, respectively. The in-medium changes in these quantities are in qualitative agreement with preliminary data from the STAR collaboration [7, 8]. For a more conclusive comparison between our model and experimental data a reliable description of the freezeout dynamics is necessary.

Towards the phase boundary, the width of the $\Delta(1232)$ further increases substantially; additional contributions from coupling to in-medium ρ-mesons (as well as pertinent vertex corrections), not included at present, are likely to accelerate the broadening (without medium effects on the ρ, the $N\rho$ channel is kinematically strongly suppressed).

Finally, in the right panel of Fig. 4, we display Δ-spectral functions in a net-baryon rich environment, approximately corresponding to heavy-ion collisions at the future GSI facility. Whereas around thermal freezeout the line shape is affected rather little, close to the phase boundary the resonance structure has essentially melted.

V. CONCLUSIONS AND OUTLOOK

Based on an effective hadronic model we have studied the properties of the nucleon and the $\Delta(1232)$ in hot and dense matter. Medium modifications in the pion cloud of the Δ were accounted for through in-medium pion and nucleon propagators (including vertex corrections), and pertinent thermal occupation factors. Direct interactions of N and Δ with thermal pions have been approximated by baryon resonances, constrained via empirical decay branchings. Within a simplified treatment we have checked that the nuclear effects on the pion lead to a Δ spectral function in cold matter which provides fair agreement with nuclear photoabsorption.

Our main result is that, under RHIC conditions, the Δ (N) spectral function exhibits significant broadening and a slight upward (downward) peak shift. In the vicinity of thermal freezeout our findings are qualitatively in line with preliminary STAR data for πN invariant-mass spectra, whereas at higher temperatures and densities the broadening becomes more extreme, reminiscent to what has been found for light vector mesons in the same framework [2].

Our work should also be considered as a step towards a comprehensive description of hadronic matter under extreme conditions, such as its equation of state [43]. Future developments will have to incorporate the coupling to vector

mesons in a chiral framework, a more complete treatment of the pion and nucleon degrees of freedom (including nonresonant interactions), as well as medium effects on excited resonances. On the phenomenological side, to address πN invariant-mass spectra in heavy-ion collisions, in-medium Δ spectral functions need to be implemented into a dynamical description of the thermal freezeout. Furthermore, the large radiative decay branching of the Δ implies that its medium modifications could play a role in electromagnetic emission spectra [44], in particular the soft-photon enhancement recently observed in central Pb-Pb collisions at the SPS [45].

Acknowledgment

[1] F. Karsch, Lect. Notes Phys. **583**, 209 (2002), URL http://arxiv.org/abs/hep-lat/0106019.
[2] R. Rapp and J. Wambach, Adv. Nucl. Phys. **25**, 1 (2000), URL http://arXiv.org/abs/hep-ph/9909229.
[3] G. Agakishiev et al. (CERES/NA45), Phys. Lett. **B422**, 405 (1998), URL http://arXiv.org/abs/nucl-ex/9712008.
[4] D. Adamova et al. (CERES/NA45), Phys. Rev. Lett. **91**, 042301 (2003), URL http://link.aps.org/abstract/PRL/v91/e042301.
[5] E. L. Hjort et al., Phys. Rev. Lett. **79**, 4345 (1997), URL http://link.aps.org/abstract/PRL/V79/P04345/.
[6] D. Pelte et al. (FOPI), Z. Phys. A **359**, 55 (1997), URL http://link.springer.de/link/service/journals/00218/bibs/7359001/73590047.htm.
[7] H.-B. Zhang (STAR) (2004), URL http://arxiv.org/abs/nucl-ex/0403010.
[8] P. Fachini, J. Phys. G **30**, S735 (2004), URL http://stacks.iop.org/0954-3899/30/S735.
[9] Y. Horikawa, M. Thies, and F. Lenz, Nucl. Phys. **A345**, 386 (1980), URL http://dx.doi.org/10.1016/0375-9474(80)90346-2.
[10] E. Oset and L. L. Salcedo, Nucl. Phys. **A468**, 631 (1987), URL http://dx.doi.org/10.1016/0375-9474(87)90185-0.
[11] T. Ericson and W. Weise, *Pions and Nuclei* (Clarendon Press, Oxford, 1988).
[12] A. B. Migdal, E. E. Saperstein, M. A. Troitsky, and D. N. Voskresensky, Phys. Rept. **192**, 179 (1990).
[13] L. H. Xia, P. J. Siemens, and M. Soyeur, Nucl. Phys. **A578**, 493 (1994), URL http://dx.doi.org/10.1016/0375-9474(94)90757-9.
[14] C. L. Korpa and M. F. M. Lutz, Nucl. Phys. **A742**, 305 (2004), URL http://arxiv.org/abs/nucl-th/0306063.
[15] C. M. Ko, L. H. Xia, and P. J. Siemens, Phys. Lett. **B231**, 16 (1989), URL http://dx.doi.org/10.1016/0370-2693(89)90104-4.
[16] C. L. Korpa and R. Malfliet, Phys. Rev. C **52**, 2756 (1995), URL http://link.aps.org/abstract/PRC/V52/P02756/.
[17] H. Leutwyler and A. V. Smilga, Nucl. Phys. **B342**, 302 (1990).
[18] C. A. Dominguez, M. Loewe, and J. C. Rojas, Phys. Lett. **B320**, 377 (1994).
[19] M. Kacir and I. Zahed, Phys. Rev. D **54**, 5536 (1996).
[20] V. L. Eletsky and B. L. Ioffe, Phys. Lett. **B401**, 327 (1997).
[21] M. Cubero, Ph.D. thesis, TH Darmstadt (1990), URL http://www-lib.kek.jp/cgi-bin/img_index?200038436.
[22] R. Rapp, M. Urban, M. Buballa, and J. Wambach, Phys. Lett. **B417**, 1 (1998), URL http://dx.doi.org/10.1016/S0370-2693(97)01360-9.
[23] M. Urban, M. Buballa, R. Rapp, and J. Wambach, Nucl. Phys. **A673**, 357 (2000), URL http://dx.doi.org/10.1016/S0375-9474(00)00125-1.
[24] J. C. Nacher, E. Oset, M. J. Vicente, and L. Roca, Nucl. Phys. **A695**, 295 (2001), URL http://dx.doi.org/10.1016/S0375-9474(01)01110-1.
[25] K. Hagiwara et al., Phys. Rev. D **66**, 01001 (2002), URL http://pdg.lbl.gov/.
[26] E. J. Moniz, Nucl. Phys. **A354**, 535c (1981), URL http://dx.doi.org/10.1016/0375-9474(81)90614-X.
[27] W. Weinhold, B. Friman, and W. Nörenberg, Phys. Lett. **B433**, 236 (1998), URL http://arxiv.org/abs/nucl-th/9710014.
[28] H. van Hees and J. Knoll, Phys. Rev. D **65**, 105005 (2002), URL http://arxiv.org/abs/hep-ph/0111193.
[29] R. Rapp and J. Wambach, Phys. Lett. **B351**, 50 (1995), URL http://dx.doi.org/10.1016/0370-2693(95)00361-N.
[30] A. B. Migdal, Rev. Mod. Phys. **50**, 107 (1978), URL http://link.aps.org/abstract/RMP/V50/P107.
[31] G. Chanfray and P. Schuck, Nucl. Phys. **A555**, 329 (1993), URL http://dx.doi.org/10.1016/0375-9474(93)90325-R.
[32] M. Herrmann, B. L. Friman, and W. Nörenberg, Nucl. Phys. **A560**, 411 (1993), URL http://dx.doi.org/10.1016/0375-9474(93)90105-7.
[33] P. Braun-Munzinger, K. Redlich, and J. Stachel (2003), URL http://arxiv.org/abs/nucl-th/0304013.
[34] R. Rapp, Phys. Rev. C **66**, 017901 (2002), URL http://link.aps.org/abstract/PRC/v66/e017901.
[35] C. L. Korpa and A. E. L. Dieperink, Phys. Rev. **C70**, 015207 (2004), URL http://arxiv.org/abs/nucl-th/0406044.

[36] J. Ahrens et al., Phys. Lett. **B146**, 303 (1984).
[37] J. Ahrens, Nucl. Phys. **A446**, 229c (1985), URL http://dx.doi.org/10.1016/0375-9474(85)90591-3.
[38] T. Frommhold et al., Phys. Lett. **B295**, 28 (1992), URL http://dx.doi.org/10.1016/0370-2693(92)90084-H.
[39] T. Frommhold et al., Z. Phys. A **350**, 249 (1994).
[40] N. Bianchi et al., Phys. Lett. **B299**, 219 (1993), URL http://dx.doi.org/10.1016/0370-2693(93)90251-C.
[41] N. Bianchi et al., Phys. Rev. C **54**, 1688 (1996), URL http://link.aps.org/abstract/PRC/V54/P01688/.
[42] H. van Hees and R. Rapp (2004), URL http://arxiv.org/abs/nucl-th/0409026.
[43] D. N. Voskresensky (2004), URL http://arxiv.org/abs/hep-ph/0402020.
[44] R. Rapp, Mod. Phys. Lett. **A19**, 1717 (2004), URL
     http://www.wspc.com.sg/journals/mpla/19/1923/S0217732304014999.html.
[45] M. M. Aggarwal et al. (WA98), Phys. Rev. Lett. **93**, 022301 (2004), URL http://arxiv.org/abs/nucl-ex/0310022.